ISSN 1560-3547, Regular and Chaotic Dynamics, 2015, Vol. 20, No. 2, pp. 134–152. © Pleiades Publishing, Ltd., 2015.

The Dynamics and Control of a Spherical Robot with an Internal Omniwheel Platform

Yury L. Karavaev[1*] and Alexander A. Kilin[2]**

[1] *M. T. Kalashnikov Izhevsk State Technical University, ul. Studencheskaya 7, Izhevsk, 426069 Russia*

[2] *Udmurt State University, ul. Universitetskaya 1, Izhevsk, 426034 Russia*

Received January 19, 2014; accepted February 27, 2015

Abstract—This paper deals with the problem of a spherical robot propelled by an internal omniwheel platform and rolling without slipping on a plane. The problem of control of spherical robot motion along an arbitrary trajectory is solved within the framework of a kinematic model and a dynamic model. A number of particular cases of motion are identified, and their stability is investigated. An algorithm for constructing elementary maneuvers (gaits) providing the transition from one steady-state motion to another is presented for the dynamic model. A number of experiments have been carried out confirming the adequacy of the proposed kinematic model.

MSC2010 numbers: 93B18, 93B52

DOI: 10.1134/S1560354715020033

Keywords: spherical robot, kinematic model, dynamic model, nonholonomic constraint, omniwheel.

1. INTRODUCTION

The motion of ball-shaped objects has long been of great interest to engineers and researchers in mechanics and dynamics. This interest is confirmed by a large number of studies devoted to both free motion [1, 2, 48–50, 52, 56, 59] and forced [3, 4, 47] motion of spherical objects. Self-propelled ball-shaped mechanical toys dating back to the late nineteenth century [5] are the prototypes of modern spherical robots. The first models of spherical robots arose at the end of the twentieth century, and more than a dozen different models implementing various motion principles were created within a few years. A detailed review and advantages of ball-shaped mobile robots with different driving mechanisms are presented in the collection of papers [6].

This paper deals with a spherical robot moving due to the motion of an omniwheel platform inside a spherical shell (see Fig. 1a). The axes of rotation of the rollers are positioned at an angle of 45° to the wheel plane. The platform moves on omniwheels whose axes of rotation of the rollers are turned through 45° relative to the wheel's plane. The omniwheels provide a higher maneuverability as compared to the conventional automobile kinematic designs. A detailed description of the design and the mathematical model of an omniwheel for rolling on a plane and a sphere is provided in [7]. We note that similar wheels can also be used for rolling on the inner surface of the sphere. However, to ensure continuity of contact between the rollers and the spherical surface, their profile needs to be adjusted.

A spherical robot design that is closest to the one considered in this paper is presented in [8]. The main difference is that the axes of rotation of the passive rollers are arranged at an angle of 90° to the axis of rotation of the wheel. In that paper, kinematic equations of motion are derived, and results of experiments involving motions in a straight line, a circle and a square are presented.

*E-mail: karavaev_yury@istu.ru

**E-mail: aka@rcd.ru

However, the error of movement of the robot was 10 to 50%, indicating a lack of consideration of the kinematic model.

Unfortunately, the dynamics of motion of a spherical robot have received little attention in the literature. Among the studies on the dynamics of spherical robots moving due to a variable gyrostatic momentum created by means of internal rotors we mention [9–14]. The motion due to the displacement of the own center of mass of the robot is dealt with in [15–20]. In the above-mentioned works, various forms of dynamical equations for spherical robots are presented and control actions for the realization of motion along typical trajectories are obtained. The thing is that the dynamics are described by nonholonomic equations. A large number of works is concerned with the derivation of these equations. Among them we mention here only the papers published over the last few years [21–24] (see also references therein). We also mention some recent studies devoted to the motion of spherical robots (or similar systems) in the presence of various resistance forces ranging from dry friction to motion in a viscous medium [46, 53–55, 57, 58].

A study of straightforward motion of the spherical robot with an internal pendulum on generic surfaces is presented in [29]. The authors have conducted numerical simulations for a spherical robot descending into a crater and moving on an inclined plane. A stability analysis and a discussion of stabilization of this model of a spherical robot taking into account the recovery of energy during deceleration are presented in [26, 30]. A control algorithm for the spherical robot of a similar design moving on an inclined plane, as well as its dynamic stabilization, is also described in [32]. A. Hartl and P. Mazzoleni [27, 28] conducted numerical simulations of the dynamics of a wind-driven spherical rover, including on rough surfaces. In [31], a novel design of the center-of-mass shifting mechanism of a spherical robot is proposed, and a kinematic model is provided along with the results of numerical simulations and experimental investigations. The design of a spherical robot with two internal pendulums is presented in [25]. In addition to dynamic equations, the authors investigate nonlinear feedback and discuss the results of numerous experiments. The results of studies presented in these papers demonstrate a significant discrepancy between theory and experimental results. This circumstance emphasizes the complexity and relevance of continuing work towards the development of control algorithms for spherical robots.

2. A MODEL OF A SPHERICAL ROBOT WITH AN INTERNAL OMNIWHEEL PLATFORM

We consider a model of a spherical robot moving on a horizontal plane as a system of bodies comprising a spherical shell of radius R_0 inside which there is a platform with three identical omniwheels of radius R_w (see Fig. 1). In this paper, by omniwheels we mean the Mecanum wheels whose design and nonholonomic model is described in [7], where an omniwheel is modeled as a flat disk for which the velocity of the point of contact with the supporting surface is directed along a straight line which forms a constant angle with the plane of the wheel.

To describe the motion of a spherical robot, we consider three coordinate systems. The first one, $OXYZ$, is a fixed system with an orthonormal basis $\boldsymbol{\alpha}, \boldsymbol{\beta}, \boldsymbol{\gamma}$; the second one, $Cx'y'z'$, is a moving system rigidly attached to the spherical shell, with an orthonormal basis $\boldsymbol{\xi}, \boldsymbol{\eta}, \boldsymbol{\zeta}$; and the third one, $Cxyz$, is a moving system rigidly attached to the omniwheel platform with an orthonormal basis $\boldsymbol{e}_1, \boldsymbol{e}_2, \boldsymbol{e}_3$ (see Fig. 1). The design of the moving platform will be described by the following constant (in the coordinate system $Cxyz$) vectors: $\boldsymbol{r_i}$ — the radius vectors of the centers of the omniwheels, $\boldsymbol{n_i}$ — the unit vectors directed along the axes of rotation of the omniwheels, $\boldsymbol{\alpha_i}$ — the unit vectors defining the directions of the axes of rotation of the rollers of each wheel at points of contact with the shell, and $\boldsymbol{r_m}$ defines the position of the center of mass of the moving omniwheel platform.

The position of the system will be described by the coordinates of the center of the spherical shell in the fixed coordinate system $\boldsymbol{r} = (x, y, 0)$, the angles of rotation of the wheels $\boldsymbol{\chi} = (\chi_1,\ \chi_2,\ \chi_3)$, and two matrices that specify the orientation of the platform and the spherical shell in space

$$\mathbf{Q} = (\boldsymbol{\alpha}, \boldsymbol{\beta}, \boldsymbol{\gamma})\,, \quad \mathbf{S} = (\boldsymbol{\xi}, \boldsymbol{\eta}, \boldsymbol{\zeta})\,.$$

Here and in the sequel (unless otherwise stated), all the vectors are referred to the axes of the coordinate system $Cxyz$ rigidly attached to the platform. Therefore, the configuration space of the system under consideration is the product of $\mathbb{R}^2 \times \mathbb{T}^3 \times SO(3) \times SO(3)$.

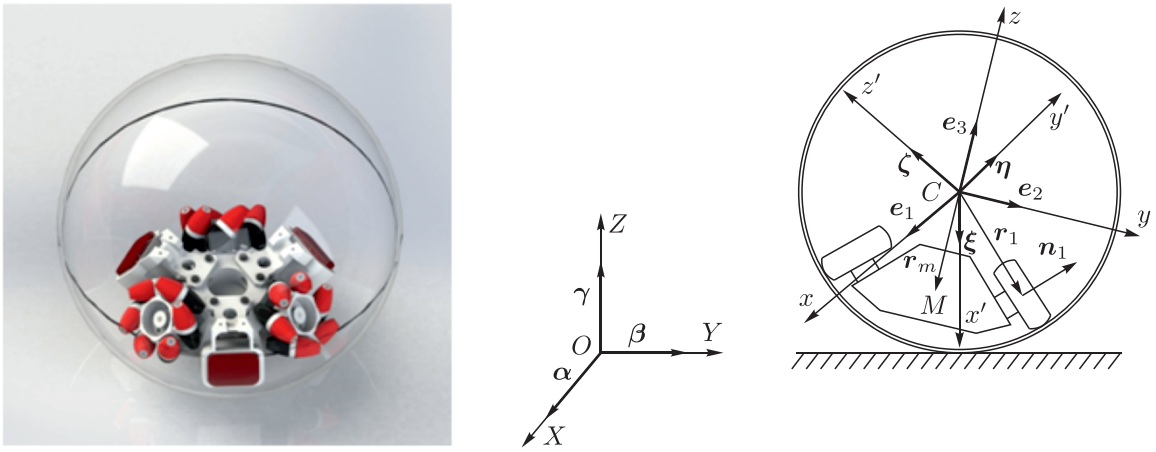

(a) (b)

Fig. 1. (a) 3D model of a spherical robot with an internal omniwheel platform, (b) schematic of a spherical robot.

In these coordinates the motion of the spherical shell and the platform is governed by the following kinematic relationships [36]

$$\dot{\boldsymbol{r}} = \mathbf{Q}^T\boldsymbol{v}, \quad \dot{\mathbf{Q}} = \widetilde{\boldsymbol{\omega}}\mathbf{Q}, \quad \dot{\mathbf{S}} = (\widetilde{\boldsymbol{\omega}} - \widetilde{\boldsymbol{\Omega}})\mathbf{S}, \tag{2.1}$$

where $\boldsymbol{v}$ is the velocity of the center of the sphere (referred to the axes of the system $Cxyz$), $\widetilde{\boldsymbol{\omega}}$ and $\widetilde{\boldsymbol{\Omega}}$ are expressed in terms of components of absolute angular velocities of the moving platform $\boldsymbol{\omega}$ and the spherical shell $\boldsymbol{\Omega}$ as follows:

$$\widetilde{\boldsymbol{\omega}} = \begin{pmatrix} 0 & \omega_3 & -\omega_2 \\ -\omega_3 & 0 & \omega_1 \\ \omega_2 & -\omega_1 & 0 \end{pmatrix}, \quad \widetilde{\boldsymbol{\Omega}} = \begin{pmatrix} 0 & \Omega_3 & -\Omega_2 \\ -\Omega_3 & 0 & \Omega_1 \\ \Omega_2 & -\Omega_1 & 0 \end{pmatrix}.$$

The variables $\boldsymbol{\omega}$, $\boldsymbol{\Omega}$ and $\boldsymbol{v}$ are quasi-velocities, and their relation to generalized velocities is given by (2.1).

We assume that there is no slipping at any point of contact of the spherical shell with the plane and the omniwheels. This leads to the imposition of nonholonomic constraints on the system. The absence of slipping of the spherical shell relative to the plane corresponds to the constraint

$$F = \boldsymbol{v} - R_0\boldsymbol{\Omega} \times \boldsymbol{\gamma} = 0, \tag{2.2}$$

while the absence of slipping of the wheels relative to the spherical shell [7] corresponds to

$$G_i = \dot{\chi}_i + \frac{R_0}{(\boldsymbol{s_i}, \boldsymbol{n_i})R_w}(\boldsymbol{\omega} - \boldsymbol{\Omega}, \mathbf{s_i}) = 0. \tag{2.3}$$

where $\boldsymbol{s_i} = \boldsymbol{r_i} \times \boldsymbol{\alpha_i}$.

An experimental model of a spherical robot with an internal omniwheel platform was created at the Laboratory of Nonlinear Analysis and the Design of New Types of Vehicles of the Udmurt State University [33, 37]. The design of this spherical robot corresponds to the following parameter values: the radius, mass and moment of inertia of the spherical shell — $R_0 = 0.15\,\text{m}$, $m_0 = 0.8\,\text{kg}$, $I_0 = 0.012\,\text{kg}\cdot\text{m}^2$; the radius of the omniwheels — $R_w = 0.07\,\text{m}$, the radius vectors defining the position of the omniwheels, the direction of their axes and the axes of the rollers: $\boldsymbol{r_i} = 0.057\,(\cos\varphi_i,\ \sin\varphi_i,\ -1)$, $\boldsymbol{n_i} = 1/\sqrt{2}\,(\cos\varphi_i,\ \sin\varphi_i,\ 1)$, $\boldsymbol{\alpha_i} = 1/\sqrt{2}\,(\cos(\varphi_i - \pi/4),\ \sin(\varphi_i - \pi/4),\ 1)$, where $\varphi_i = 2\pi(i-1)/3$, $i = 1\ldots3$; the mass and the tensor

of the moving omniwheel platform — $m = 2.5\,\text{kg}$, $\mathbf{I} = \text{diag}(0.016,\ 0.016,\ 0.023)\,\text{kg}\cdot\text{m}^2$. All experimental studies have been conducted using this specimen, and the numerical calculations found below have been carried out for the specified parameter values.

We consider the problem of controlling a spherical robot in the following formulation:

> ***determine a control action required to implement the motion along a given trajectory $x(t), y(t)$ at $t \in [0,\ T]$ with a predetermined time dependence of the projection of the angular velocity of the spherical shell on the vertical $\Omega_\gamma(t)$ for known initial orientations $\alpha(0)$, $\beta(0)$, $\gamma(0)$ and the angular velocity of the platform $\omega(0)$.***

This problem can be solved in the framework of two different models: the kinematic model and the dynamic model. We first consider the simpler kinematic model.

3. CONTROL IN THE FRAMEWORK OF THE KINEMATIC MODEL

Within the framework of the kinematic model we will use the angular velocities of the rotating omniwheels $\dot\chi_i$ as the control actions. Expressing from the constraint equation

$$\boldsymbol{\Omega} = \frac{1}{R}\boldsymbol{\gamma} \times \boldsymbol{v} + \Omega_\gamma \boldsymbol{\gamma}$$

and substituting the resulting expression in Eq. (2.3) taking into account Eq. (2.1), we determine the dependence of control actions on the given trajectory $(\boldsymbol{r}_c(t), \Omega_\gamma(t))$ and the variables of the system under consideration $(\mathbf{Q}, \boldsymbol{\omega})$

$$\dot\chi_i = \frac{1}{R_w}\frac{(\boldsymbol{s_i}, \boldsymbol{\gamma} \times \mathbf{Q}\dot{\boldsymbol{r}}_c + R_0\Omega_\gamma\boldsymbol{\gamma} - R_0\boldsymbol{\omega})}{(\boldsymbol{s_i}, \boldsymbol{n_i})}. \tag{3.1}$$

We make the following assumption.

Assumption. *Within the framework of the kinematic (quasi-static) model we shall assume that during motion of the spherical robot the center of mass of the platform is always in the lowest possible position. The radius vector of the center of mass can be expressed as*

$$\boldsymbol{r_m} = -R_m\boldsymbol{\gamma},$$

where R_m is the distance from the origin of the moving coordinate system to the center of mass of the moving platform.

It follows from this assumption that the angular velocity $\boldsymbol{\omega}$ is perpendicular to the plane on which the spherical robot moves, i.e.,

$$\boldsymbol{\omega} = \omega_\gamma\boldsymbol{\gamma}. \tag{3.2}$$

Furthermore, if we write the matrix $\mathbf{Q}$ in terms of Euler angles it is easy to show that in this case the angles of nutation and self-rotation are constant $\theta = \theta_m$, $\varphi = \varphi_m$ and define up to sign the spherical coordinates of the center of mass of the omniwheel platform in the moving coordinate system. Decomposing the matrix $\mathbf{Q}$ into the corresponding constant multipliers, we get

$$\mathbf{Q} = \mathbf{Q}_m\mathbf{Q}_\psi, \tag{3.3}$$

where the matrix $\mathbf{Q}_m$ has the form

$$\mathbf{Q}_m = \begin{pmatrix} \cos\varphi_m & \cos\theta_m\sin\varphi_m & \sin\theta_m\sin\varphi_m \\ -\sin\varphi_m & \cos\theta_m\cos\varphi_m & \sin\theta_m\cos\varphi_m \\ 0 & -\sin\theta_m & \cos\theta_m \end{pmatrix},$$

and the matrix

$$\mathbf{Q}_\psi = \begin{pmatrix} \cos\psi & \sin\psi & 0 \\ -\sin\psi & \cos\psi & 0 \\ 0 & 0 & 1 \end{pmatrix}$$

corresponds to the rotation of the moving platform about the vertical axis through the precession angle ψ. The vector $\boldsymbol{\gamma}$ can be expressed as

$$\boldsymbol{\gamma} = \mathbf{Q}_m \boldsymbol{e}_3, \tag{3.4}$$

and the vertical projection of the angular velocity of the platform is equal to the derivative of the precession angle $\omega_\gamma = \dot{\psi}$.

Substituting (3.2), (3.3) and (3.4) into the expression for the calculation of control actions (3.1), we come to the conclusion that the following proposition holds.

Proposition 1. *The dependence of the angular velocities of rotation of the wheels required for the motion along the trajectory $\boldsymbol{r}_c(t)$ for a given function $\Omega_\gamma(t)$ has the following form*

$$\dot{\chi}_i = \frac{1}{R_w} \frac{(\mathbf{Q}_m^T \boldsymbol{s_i}, \boldsymbol{e}_3 \times \mathbf{Q}_\psi^T \dot{\boldsymbol{r}}_c + R_0(\Omega_\gamma - \omega_\gamma)\boldsymbol{e}_3)}{(\boldsymbol{s_i}, \boldsymbol{n_i})}, \tag{3.5}$$

where the angular velocity ω_γ is a free parameter. That is, within the kinematic model the motion along a given trajectory can be implemented up to an arbitrary rotation of the platform about the vertical axis $\omega_\gamma(t)$.

Experimental investigations of the motion of the full-scale specimen have shown that at low velocities the sphere virtually does not rotate about the vertical axis, so we will consider the motion in the framework of the rubber rolling model [38–41], that is, we will assume that $\Omega_\gamma \equiv 0$.

3.1. Particular Cases

Next, we consider some particular cases of motion within the framework of the kinematic model.

The motion with constant control actions. We consider the motion of the spherical robot in the framework of the rubber rolling model with constant control actions, i.e.,

$$\dot{\boldsymbol{\chi}} = \text{const}.$$

It follows from the constraint equation (2.3) that during constant control the vector of relative angular velocity also remains constant $\widehat{\boldsymbol{\omega}} = \boldsymbol{\omega} - \boldsymbol{\Omega} = \text{const}$. Taking into account that the motion under consideration is quasi-static ($\boldsymbol{r_m} \parallel \boldsymbol{\gamma},\ \boldsymbol{\omega} \parallel \boldsymbol{\gamma}$), the no-slip condition of the spherical shell (2.2) can be written as

$$\boldsymbol{v} = \frac{R_0}{R_m} \boldsymbol{r_m} \times \widehat{\boldsymbol{\omega}}.$$

Moreover, taking into account the absence of slipping in the rubber rolling model ($\Omega_\gamma \equiv 0$), it is easy to show that

$$\boldsymbol{\omega} = \frac{1}{R_m^2} (\boldsymbol{r_m}, \widehat{\boldsymbol{\omega}}) \boldsymbol{r_m}.$$

Therefore, the vectors of velocity of the spherical robot and the angular velocity vector of the platform in the moving coordinate system remain constant.

Using these equations, as well as the fact that the vectors $\boldsymbol{\omega}$ and $\boldsymbol{v}$ are perpendicular (which follows from the quasi-static condition), we can calculate the radius of curvature of the trajectory along which the spherical robot is moving

$$\frac{1}{\rho} = \frac{|\ \boldsymbol{V} \times \dot{\boldsymbol{V}}\ |}{|\ \boldsymbol{V}\ |^3} = \frac{|\ \mathbf{Q}^T \boldsymbol{v} \times \mathbf{Q}^T (\boldsymbol{\omega} \times \boldsymbol{v})\ |}{|\ \mathbf{Q}^T \boldsymbol{v}\ |^3} = \frac{1}{R_0} \frac{(\widehat{\boldsymbol{\omega}}, \boldsymbol{r_m})}{\sqrt{\widehat{\boldsymbol{\omega}}^2 \boldsymbol{r_m}^2 - (\widehat{\boldsymbol{\omega}}, \boldsymbol{r_m})^2}}. \tag{3.6}$$

As can be seen from Eq. (3.6), the radius of curvature of the trajectory of motion is constant. Therefore, since Eq. (3.6) is homogeneous in $\widehat{\boldsymbol{\omega}}$ and $\widehat{\boldsymbol{\omega}}$ is linearly dependent on $\boldsymbol{\chi}$, the following proposition holds.

Proposition 2. *With constant control actions* $\dot{\boldsymbol{\chi}} = \text{const}$ *the spherical robot moves uniformly in a circle whose radius is given by Eq.* (3.6) *and is dependent only on the ratio of control actions* χ_i/χ_j.

The motion in a straight line. Analyzing Eq. (3.6), we can conclude that the motion in a straight line ($\rho = \infty$) is possible in the case $\boldsymbol{\omega} = 0$. Consequently, by virtue of Eqs. (2.1), the motion in a straight line does not involve any change in the orientation of the platform, i.e., $\psi = \text{const}$. Using this fact, as well as the no-spin requirement of the rubber rolling model, the control actions required for the spherical robot to move with velocity v in a straight line directed at the angle δ to the axis OX with the platform orientation ψ can be written as

$$\dot{\chi}_i = \frac{(\mathbf{Q}_m^T \boldsymbol{s_i} \times \boldsymbol{e}_3, \mathbf{Q}_\psi \boldsymbol{V})}{R_w(\boldsymbol{s_i}, \boldsymbol{n_i})}, \tag{3.7}$$

where $\boldsymbol{V} = (v\cos(\delta),\ v\sin(\delta),\ 0)$.

We note that in order to calculate the control actions (3.5), (3.7), we need to define the position of the center of mass of the platform. To do so requires the development of sophisticated and high-precision equipment. At the same time, the motion of the spherical robot without feedback sensors requires that either these parameters are determined or that the moving platform is balanced.

Determination of displacement of the center of mass of the moving platform. The displacement of the center of mass of the platform can also be calculated from the results of several test experiments involving the motion of the spherical robot with constant control actions. Indeed, we note that the radii of the circles along which the spherical robot moves with constant controls are related with the radius vector of the center of mass by the ratio (3.6). Moreover, these ratios depend only on the direction of displacement (the angles φ_m and θ_m) and are not dependent on the value of displacement. Consequently, a system of two equations such as Eq. (3.6) for various control actions is sufficient to determine the direction of displacement of the center of mass of the moving platform. Thus, to calculate the direction of displacement of the center of mass (φ_m and θ_m) we need to conduct two experiments involving spherical robot motion with various constant control actions and measure the radii of the circles along which the spherical robot moves. For the developed experimental specimen these values were equal to

$$\varphi_m = 1.521 \pm 0.018,\ \theta_m = 0.0535 \pm 0.0075. \tag{3.8}$$

This technique was used in [33] for the experimental determination of displacement of the center of mass of a prototype of the spherical robot with an internal omniwheel platform. As the experiments have shown, the correct implementation of motion along a predetermined trajectory essentially requires that the displacement of the center of mass be taken into account. An example of experimental trajectories of the spherical robot with controls calculated for the **rectilinear** motion taking into account and ignoring the displacement of the center of mass is shown in Fig. 2a. The heavy lines in the figure show the circles with their radii averaged from the results of ten experiments for each of the control options. As shown in Fig. 2a, even a small (about 3 degrees) displacement of the center of mass leads to a more than twofold decrease in the radius of curvature of the resulting trajectory.

The motion in a circle. As mentioned above, in the general case the trajectory of motion under constant control actions is a circle whose radius is determined by the ratio of the angular velocities of the wheels of the spherical robot and the center of mass displacement. In the framework of the kinematic model the radius is not dependent on the absolute values of control actions (they determine only the velocity of motion along the trajectory).

Let us investigate the dependence of the radius of the trajectory on the absolute values of control actions. To this end, we choose as the base case the motion with the following control actions

$$\dot{\chi}_1 = -14.28,\ \dot{\chi}_2 = 28.57,\ \dot{\chi}_3 = 57.14. \tag{3.9}$$

The corresponding radius of curvature of the trajectory, calculated using Eq. (3.6) and taking into account the displacement of the center of mass (3.8), is $\rho = 100.08$ mm. Examples of the trajectory

are shown in Fig. 2b. The heavy line in the figure shows a circle with a radius averaged from the results of five experiments. We carried out five series of experiments with control actions greater than the base case (3.9) by $\kappa = 1 \dots 5$ times. The resulting experimental dependence of the radius of the trajectory on the coefficient κ is shown in Fig. 2c. The horizontal straight line corresponds to the theoretical value of the radius of the circle calculated for the controls (3.9) in the framework of the kinematic model. The region shown in gray indicates the confidence interval of the radius of curvature for a 95% probability.

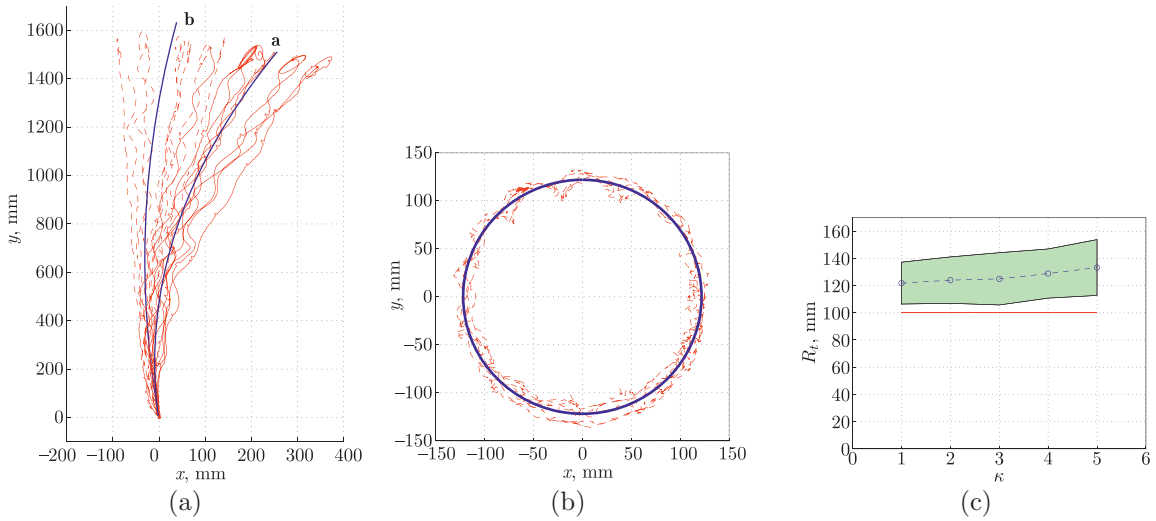

Fig. 2. Trajectories of the spherical robot with controls calculated (a) for the rectilinear motion: **a** ignoring the displacement of the center of mass, **b** taking into account the displacement of the center of mass; (b) for constant control actions. (c) Dependence of the radius of curvature of the trajectory on the angular velocity of motion along the trajectory with constant control actions.

As shown in Fig. 2, as the velocity of motion increases, the deviation from the kinematic model also increases, which limits its application. To achieve a higher speed of motion requires investigating the dynamic model.

4. CONTROL IN THE FRAMEWORK OF THE DYNAMIC MODEL

4.1. Equations of Motion

Let us now consider the problem of controlling a spherical robot taking into account its dynamics. For the model of a spherical robot described above, we will write the equations of motion in quasi-velocities ($\boldsymbol{\omega}$, $\boldsymbol{\Omega}$, $\boldsymbol{v}$, $\dot{\boldsymbol{\chi}}$) taking into account the nonholonomic constraints and controls

$$\begin{gathered}
\frac{d}{dt}\left(\frac{\partial L}{\partial \boldsymbol{\omega}}\right) = \frac{\partial L}{\partial \boldsymbol{\omega}} \times \boldsymbol{\omega} + \frac{\partial L}{\partial \boldsymbol{v}} \times \boldsymbol{v} + \frac{\partial L}{\partial \boldsymbol{\gamma}} \times \boldsymbol{\gamma} + \left(\frac{\partial \boldsymbol{G}}{\partial \boldsymbol{\omega}}\right)^T \widetilde{\boldsymbol{\lambda}}, \\
\frac{d}{dt}\left(\frac{\partial L}{\partial \boldsymbol{\Omega}}\right) = \frac{\partial L}{\partial \boldsymbol{\Omega}} \times \boldsymbol{\omega} + \left(\frac{\partial \boldsymbol{G}}{\partial \boldsymbol{\Omega}}\right)^T \widetilde{\boldsymbol{\lambda}} + \left(\frac{\partial \boldsymbol{F}}{\partial \boldsymbol{\Omega}}\right)^T \boldsymbol{\lambda}, \\
\frac{d}{dt}\left(\frac{\partial L}{\partial \boldsymbol{v}}\right) = \frac{\partial L}{\partial \boldsymbol{v}} \times \boldsymbol{\omega} + \left(\frac{\partial \boldsymbol{F}}{\partial \boldsymbol{v}}\right)^T \boldsymbol{\lambda}, \\
\frac{d}{dt}\left(\frac{\partial L}{\partial \dot{\chi}}\right) = \frac{\partial L}{\partial \chi} + \left(\frac{\partial \boldsymbol{G}}{\partial \dot{\chi}}\right)^T \widetilde{\boldsymbol{\lambda}} + \boldsymbol{K}.
\end{gathered} \tag{4.1}$$

Here L is the Lagrangian function, $\boldsymbol{\lambda} = (\lambda_1, \lambda_2, \lambda_3)$ and $\widetilde{\boldsymbol{\lambda}} = (\widetilde{\lambda}_1, \widetilde{\lambda}_2, \widetilde{\lambda}_3)$ are undetermined Lagrange multipliers, $\boldsymbol{K} = (K_1, K_2, K_3)$ is the vector of control torques where K_i is the torque applied to the axis of the i-th wheel, and $\boldsymbol{F}$ and $\boldsymbol{G}$ are the nonholonomic constraints (2.2) and (2.3). A more detailed description of how the equations of motion were derived can be found in [36].

The kinetic energy of the system can be represented as the sum of three terms: the kinetic energy of the spherical shell T_0, the kinetic energy of the platform T_p and the kinetic energy of the wheels T_i

$$T = T_0 + T_p + \sum_{i=1}^{3} T_i.$$

The kinetic energy of the spherical shell and the moving platform has the following form:

$$T_0 = \frac{1}{2} m_0 \boldsymbol{v}^2 + \frac{1}{2} I_0 \boldsymbol{\Omega}^2,$$

$$T_p = \frac{1}{2} m_p \boldsymbol{v}^2 + \frac{1}{2} (\boldsymbol{\omega}, \mathbf{I_p}\boldsymbol{\omega}) + m_p (\boldsymbol{v}, \boldsymbol{\omega} \times \boldsymbol{r_p}),$$

where m_0 and I_0 are the mass and the central tensor of inertia of the spherical shell, m_p and $\mathbf{I_p}$ are the mass of the moving platform and its tensor of inertia relative to the center of the sphere, and $\boldsymbol{r_p}$ is the radius vector from the center of the sphere to the center of mass of the platform (without the omniwheels). The kinetic energy of each of the wheels has the following form:

$$T_i = \frac{1}{2} m_i \boldsymbol{v}^2 + m_i (\boldsymbol{v}, \boldsymbol{\omega} \times \boldsymbol{r_i}) + \frac{1}{2} (\boldsymbol{\omega}, \mathbf{I_i}\boldsymbol{\omega}) + j(\boldsymbol{\omega}, \boldsymbol{n_i})\dot{\chi}_i + \frac{1}{2} j \dot{\chi}_i^2,$$

where m_i and $\mathbf{I_i}$ are the mass of the i-th wheel and its tensor of inertia relative to the point C, and j is the axial moment of inertia of the wheels. The total kinetic energy of the system can be represented as

$$T = \frac{1}{2}(m + m_0)\boldsymbol{v}^2 + \frac{1}{2} I_0 \boldsymbol{\Omega}^2 + \frac{1}{2}(\boldsymbol{\omega}, \mathbf{I}\boldsymbol{\omega}) + m(\boldsymbol{v}, \boldsymbol{\omega} \times \boldsymbol{r_m}) + \sum_{i=1}^{3} j\dot{\chi}_i (\boldsymbol{\omega}, \boldsymbol{n_i}) + \frac{1}{2} \sum_{i=1}^{3} j \dot{\chi}_i^2, \tag{4.2}$$

where

$m = m_p + \sum\limits_{i=1}^{3} m_i$ is the mass of the moving platform with omniwheels,

$\boldsymbol{r_m} = \dfrac{m_p \boldsymbol{r_p} + \sum\limits_{i=1}^{3} m_i \boldsymbol{r_i}}{m}$ is the radius vector of the center of mass of the moving platform with omniwheels,

$\mathbf{I} = \mathbf{I_p} + \sum\limits_{i=1}^{3} \mathbf{I_i}$ is the tensor of inertia of the moving platform with omniwheels relative to the center of the sphere.

In this notation, the potential energy of the system can be expressed as

$$U = mg(\boldsymbol{r_m}, \boldsymbol{\gamma}), \tag{4.3}$$

where g is the gravitational acceleration.

Defining the Lagrangian $L = T - U$ by means of Eqs. (4.2) and (4.3) and substituting it into Eqs. (4.1), we get

$$\begin{gathered}
\mathbf{I}\dot{\boldsymbol{\omega}} + m(\boldsymbol{r_m} \times \dot{\boldsymbol{v}}) + \sum_{i=1}^{3} j\ddot{\chi}_i \boldsymbol{n_i} + \boldsymbol{\omega} \times \left(\mathbf{I}\boldsymbol{\omega} + m(\boldsymbol{r_m} \times \boldsymbol{v}) + \sum_{i=1}^{3} j\dot{\chi}_i \boldsymbol{n_i} \right) + m\boldsymbol{v} \times (\boldsymbol{r_m} \times \boldsymbol{\omega}) \\
= \sum_{i=1}^{3} k_i \boldsymbol{s_i} \lambda_i - mg(\boldsymbol{r_m} \times \boldsymbol{\gamma}), \\
I_0 \dot{\boldsymbol{\Omega}} + \boldsymbol{\omega} \times I_0 \boldsymbol{\Omega} = -(R_0 \boldsymbol{\gamma}) \times \widetilde{\boldsymbol{\lambda}} - \sum_{i=1}^{3} k_i \boldsymbol{s_i} \lambda_i, \\
(m + m_0)\dot{\boldsymbol{v}} + m(\dot{\boldsymbol{\omega}} \times \boldsymbol{r_m}) + \boldsymbol{\omega} \times ((m_0 + m)\boldsymbol{v} + m(\boldsymbol{\omega} \times \boldsymbol{r_m})) = \widetilde{\boldsymbol{\lambda}}, \\
j\ddot{\chi}_i + j(\dot{\boldsymbol{\omega}}, \boldsymbol{n_i}) = \lambda_i + K_i,
\end{gathered} \tag{4.4}$$

where $k_i = \dfrac{R_0}{R_w(\boldsymbol{s_i}, \boldsymbol{n_i})}$. We find the undetermined multipliers from the last two Eqs. (4.4) and the time derivative of the constraint equations (2.3)

$$\lambda_i = jk_i(\dot{\boldsymbol{\Omega}} - \dot{\boldsymbol{\omega}}, \boldsymbol{s_i}) + j(\dot{\boldsymbol{\omega}}, \boldsymbol{n_i}) - K_i,\ i = 1 \dots 3,$$
$$\widetilde{\boldsymbol{\lambda}} = (m + m_0)\dot{\boldsymbol{v}} + m(\dot{\boldsymbol{\omega}} \times \boldsymbol{r_m}) + \boldsymbol{\omega} \times ((m_0 + m)\boldsymbol{v} + m(\boldsymbol{\omega} \times \boldsymbol{r_m})).$$

Substituting them into the equations of motion and using the constraint equations (2.2) and (2.3) to eliminate $\dot{\chi}_i$ and $\boldsymbol{v}$, we get

$$\begin{gathered}(\mathbf{I} + \mathbf{J_{ss}} - \mathbf{J_{ns}} - \mathbf{J_{sn}})\dot{\boldsymbol{\omega}} + (\mathbf{J_{ns}} - \mathbf{J_{ss}} + mR_0((\boldsymbol{\gamma}, \boldsymbol{r_m}) - \boldsymbol{\gamma} \otimes \boldsymbol{r_m}))\dot{\boldsymbol{\Omega}} \\ = -\sum_{i=1}^{3} k_i \mathbf{s_i} K_i - \boldsymbol{\omega} \times \mathbf{I}\boldsymbol{\omega} + (\mathbf{J_{ns}}(\boldsymbol{\Omega} - \boldsymbol{\omega})) \times \boldsymbol{\omega} - mR_0 \boldsymbol{r_m} \times (\boldsymbol{\gamma} \times (\boldsymbol{\Omega} \times \boldsymbol{\omega})) - mg(\boldsymbol{r_m} \times \boldsymbol{\gamma}) \\ (\mathbf{J_{sn}} - \mathbf{J_{ss}} + mR_0((\boldsymbol{r_m}, \boldsymbol{\gamma}) - \boldsymbol{r_m} \otimes \boldsymbol{\gamma}))\dot{\boldsymbol{\omega}} + (I_0 + \mathbf{J_{ss}} + (m + m_0){R_0}^2(\boldsymbol{\gamma}^2 - \boldsymbol{\gamma} \otimes \boldsymbol{\gamma}))\dot{\boldsymbol{\Omega}} \\ = -(m + m_0){R_0}^2 \boldsymbol{\gamma} \times (\boldsymbol{\gamma} \times (\boldsymbol{\Omega} \times \boldsymbol{\omega})) - mR_0(\boldsymbol{\gamma} \times (\boldsymbol{\omega} \times (\boldsymbol{\omega} \times \boldsymbol{r_m}))) - I_0 \boldsymbol{\omega} \times \boldsymbol{\Omega} + \sum_{i=1}^{3} k_i \boldsymbol{s_i} K_i,\end{gathered} \tag{4.5}$$

where we have used the notation $\mathbf{J_{ss}} = \sum\limits_{i=1}^{3} jk_i{}^2(\boldsymbol{s_i} \otimes \boldsymbol{s_i})$, $\mathbf{J_{sn}} = \sum\limits_{i=1}^{3} jk_i(\boldsymbol{s_i} \otimes \boldsymbol{n_i})$, $\mathbf{J_{ns}} = \sum\limits_{i=1}^{3} jk_i(\boldsymbol{n_i} \otimes \boldsymbol{s_i})$, and the tensor product of the vectors $\boldsymbol{a}$ and $\boldsymbol{b}$ is defined as follows:

$$\boldsymbol{a} \otimes \boldsymbol{b} = \|a_i b_j\|.$$

Together with the Poisson equation (one of Eqs. (2.1))

$$\dot{\boldsymbol{\gamma}} = \boldsymbol{\gamma} \times \boldsymbol{\omega} \tag{4.6}$$

Eqs. (4.5) form a closed reduced system of equations.

This system admits two first integrals of motion

$$\boldsymbol{\gamma}^2 = 1,\ (\boldsymbol{M}, \boldsymbol{\gamma}) = M_\gamma = \text{const}, \tag{4.7}$$

where the vector $\boldsymbol{M}$ has the form

$$\begin{aligned}\boldsymbol{M} = {} & (\mathbf{I} - \mathbf{J_{ns}} + mR_0((\boldsymbol{\gamma}, \boldsymbol{r_m}) - \boldsymbol{r_m} \otimes \boldsymbol{\gamma}))\boldsymbol{\omega} \\ & + (I_0 + \mathbf{J_{ns}} + mR_0((\boldsymbol{\gamma}, \boldsymbol{r_m}) - \boldsymbol{\gamma} \otimes \boldsymbol{r_m}) + (m + m_0){R_0}^2(1 - \boldsymbol{\gamma} \otimes \boldsymbol{\gamma}))\boldsymbol{\Omega}.\end{aligned} \tag{4.8}$$

In the case of free motion ($\boldsymbol{K} = 0$) the integrals (4.7) are supplemented by the energy integral, which, after substituting the constraint equations (2.2) and (2.3) into Eq. (4.2), takes the following form:

$$\begin{aligned}\mathcal{E} = {} & \frac{1}{2}(m + m_0)R_0^2(\boldsymbol{\Omega} \times \boldsymbol{\gamma})^2 + \frac{1}{2}I_0\boldsymbol{\Omega}^2 + \frac{1}{2}(\boldsymbol{\omega}, \mathbf{I}\boldsymbol{\omega}) + mR_0(\boldsymbol{\Omega} \times \boldsymbol{\gamma}, \boldsymbol{\omega} \times \boldsymbol{r_m}) \\ & + (\boldsymbol{\Omega} - \boldsymbol{\omega}, \mathbf{J_{sn}}\boldsymbol{\omega}) + \frac{1}{2}(\boldsymbol{\Omega} - \boldsymbol{\omega}, \mathbf{J_{ss}}(\boldsymbol{\Omega} - \boldsymbol{\omega})) + mg(\boldsymbol{r_m}, \boldsymbol{\gamma}).\end{aligned} \tag{4.9}$$

Thus, even in the case of free motion the phase flow in the nine-dimensional space $(\boldsymbol{\omega}, \boldsymbol{\Omega}, \boldsymbol{\gamma})$ is foliated by six-dimensional level sets of the integrals (4.7) and (4.9), and in the general case is apparently nonintegrable. Therefore, it appears to be interesting to look for integrable cases of the system (4.5)–(4.6) and its particular solutions. We note that in the general case the free motion governed by the nonholonomic system (4.5)–(4.6) may be quite complex and include elements of both Hamiltonian and dissipative behavior. In particular, both simple and complex attracting (repelling) sets, including various types of strange attractors, can be observed in the system. Such behavior in simpler systems with nonholonomic constraints was mentioned in [2, 14, 39, 42–45, 51].

Remark. The equation of motion for the vector $\boldsymbol{M}$ is independent of control actions and has the form

$$\dot{\boldsymbol{M}} = \boldsymbol{M} \times \boldsymbol{\omega} - mg(\boldsymbol{r_m} \times \boldsymbol{\gamma}).$$

Expressing $\boldsymbol{\Omega}$ as a function of $\boldsymbol{\omega}$ and $\boldsymbol{M}$ from Eq. (4.8) and substituting it into the equation of motion, we can obtain a closed system in terms of the variables $\boldsymbol{\omega}$, $\boldsymbol{M}$ and $\boldsymbol{\gamma}$. However, the resulting equation for $\dot{\boldsymbol{\omega}}$ is too cumbersome, therefore we are not providing it here. We also note that in the case when there is no force of gravity the vector $\boldsymbol{M}$ is conserved in the absolute space and is apparently a generalization of the conserved vector of the angular momentum relative to the point of contact in the simpler problems of spherical bodies rolling on a plane [9, 10, 34, 35].

4.2. Particular Solutions

Let us next find the fixed points of the system (4.5)–(4.6) that are its simplest particular solutions. Prior to searching for fixed points of the system, we will prove a simple proposition about the motion of a spherical robot in the absolute space corresponding to the fixed points of the reduced system.

Proposition 3. *Let $\boldsymbol{\omega}_0, \boldsymbol{\Omega}_0, \boldsymbol{\gamma}_0$ be a fixed point of the reduced system* (4.5)–(4.6)*, then in the absolute space it corresponds to motion along a trajectory with a constant radius of curvature*

$$\frac{1}{\rho} = \frac{\sqrt{\boldsymbol{v}_0^2\boldsymbol{\omega}_0^2 - (\boldsymbol{\omega}_0, \boldsymbol{v}_0)^2}}{\boldsymbol{v}_0^2}, \tag{4.10}$$

where

$$\boldsymbol{v}_0 = R_0\boldsymbol{\Omega}_0 \times \boldsymbol{\gamma}_0. \tag{4.11}$$

Proof. We first note that it follows from the no-slip condition (2.2) that with constant vectors $\boldsymbol{\Omega}$ and $\boldsymbol{\gamma}$ the velocity of the spherical robot (4.11) referred to the axes of the moving coordinate system is constant.

We express the velocity of the spherical robot $\boldsymbol{V}$ and its derivative in the fixed coordinate system $OXYZ$: $\boldsymbol{V} = \mathbf{Q}^T\boldsymbol{v}$, $\dot{\boldsymbol{V}} = \mathbf{Q}^T(\dot{\boldsymbol{v}} + \boldsymbol{\omega} \times \boldsymbol{v})$. Substituting these relations into the expression for calculating the radius of curvature (the first equation of (3.6)) and taking into account (4.11), we obtain (4.10) for the radius of curvature of the trajectory.

Remark. A similar proposition holds for arbitrary systems governing the rolling of spherical bodies on a plane. The only thing that changes is the dependence of velocity $\boldsymbol{v_0}$ on the variables of the reduced system. In particular, the angular velocities $\boldsymbol{\omega}$ and $\boldsymbol{\Omega}$ coincide in systems without internal mechanisms such as a ball with a displaced center of mass, hence $\boldsymbol{v} = -R_0\dot{\boldsymbol{\gamma}}$, that is, the ball is stationary (possibly rotating around the vertical axis).

Let us find the fixed points of the reduced system (4.5)–(4.6) for free motion that correspond to steady-state motions of the spherical robot in the absolute space. Substituting $\dot{\boldsymbol{\Omega}} = 0, \dot{\boldsymbol{\omega}} = 0, \boldsymbol{K} = 0$ into Eqs. (4.6), we obtain a system of algebraic equations for determining these fixed points

$$\begin{gathered}(\mathbf{I}\boldsymbol{\omega} + \mathbf{J_{ns}}(\boldsymbol{\Omega} - \boldsymbol{\omega}) + mR_0(\boldsymbol{r_m}, \boldsymbol{\gamma})\boldsymbol{\Omega}) \times \boldsymbol{\omega} - (mR_0(\boldsymbol{\gamma}, \boldsymbol{\omega})\boldsymbol{\Omega} - mg\boldsymbol{\gamma}) \times \boldsymbol{r_m} = 0 \\ \big((m + m_0){R_0}^2\boldsymbol{\gamma} \times (\boldsymbol{\Omega} \times \boldsymbol{\omega}) + mR_0\boldsymbol{\omega} \times (\boldsymbol{\omega} \times \boldsymbol{r_m})\big) \times \boldsymbol{\gamma} - I_0\boldsymbol{\omega} \times \boldsymbol{\Omega} = 0 \\ \boldsymbol{\gamma} \times \boldsymbol{\omega} = 0.\end{gathered} \tag{4.12}$$

The system (4.12) has the following solutions.

1. Two three-parameter families of fixed points:

$$\boldsymbol{\omega} = 0,\ \boldsymbol{\Omega} = \boldsymbol{\Omega}_0,\ \boldsymbol{\gamma} = \pm\frac{\boldsymbol{r_m}}{|\boldsymbol{r_m}|}. \tag{4.13}$$

This solution corresponds to motions of the spherical robot where the center of mass of the platform is located in the lowest (highest) possible point, its orientation does not change with time, the spherical shell rotates with constant angular velocity $\boldsymbol{\Omega}_0$, and the center of the spherical robot

either remains stationary (with $\boldsymbol{\Omega}_0 \parallel \boldsymbol{\gamma}$) or moves in a straight line (with $\boldsymbol{\Omega}_0 \nparallel \boldsymbol{\gamma}$). Note that since the nonholonomic constraint (2.3) is unilateral, no solution with the "+" sign can be realized in practice.

2. A two-parameter family of fixed points defined by the following relations:

$$\begin{gathered}\boldsymbol{\omega} = \omega\boldsymbol{\gamma},\ \boldsymbol{\Omega} = \omega C_1\boldsymbol{\gamma} - \omega\frac{mR_0}{J_0}\boldsymbol{r_m},\\ \boldsymbol{\gamma} = -\frac{\mathbf{A^{-1}}\boldsymbol{b} + \boldsymbol{r_m}\times(\mathbf{A^{-1}}\boldsymbol{r_m}\times\mathbf{A^{-1}}\boldsymbol{b})}{1-(\boldsymbol{r_m},\mathbf{A^{-1}}\boldsymbol{r_m})},\end{gathered} \tag{4.14}$$

where

$$\mathbf{A} = \frac{J_0}{m^2R_0^2}\left(\mathbf{I} + (C_1-1)\mathbf{J_{ns}} - C_2\right),\ \boldsymbol{b} = \frac{J_0}{m^2R_0^2}\left(mR_0C_1 - \frac{mg}{\omega^2} - \frac{R_0}{J_0}\mathbf{J_{ns}}\right)\boldsymbol{r_m},$$

$J_0 = I_0 + (m+m_0){R_0}^2$, and C_1, C_2 and ω are the parameters of the family, two of which can be regarded as independent, and the third one can be calculated from the condition $\boldsymbol{\gamma}^2 = 1$. The independent parameters can be expressed in terms of the integrals of motion M_γ and $\mathcal{E}$ by substituting (4.14) into the corresponding equations. Further analysis of the fixed points can be aimed at investigating the solvability of the resulting system of equations and identifying regions of existence of solutions of (4.13) and (4.14) in the space of first integrals. This matter is quite complex. It requires separate consideration and is beyond the scope of this study. Note that in the absolute coordinate system the solutions of (4.14) correspond to the rolling of the spherical robot in a circle of radius

$$\rho = \frac{mR_0}{J_0}\sqrt{\boldsymbol{r_m}^2 - (\boldsymbol{r_m},\boldsymbol{\gamma})^2},$$

where $\boldsymbol{\gamma}$ is expressed from the second equation (4.14).

4.3. Stability of Motion in a Straight Line

We now consider the question of linear stability of the particular solution (4.13). To do this, we linearize the system (4.5)–(4.6) near this solution and obtain a system of linear differential equations with constant coefficients of the form

$$\mathbf{A}\dot{\boldsymbol{z}} = \mathbf{B}\boldsymbol{z}, \tag{4.15}$$

where $\boldsymbol{z} = (\omega_1,\ \omega_2,\ \omega_3,\ \Omega_1 - \Omega_{0_1},\ \Omega_2 - \Omega_{0_2},\ \Omega_3 - \Omega_{0_3},\ \gamma_1 - \gamma_{0_1},\ \gamma_2 - \gamma_{0_2},\ \gamma_3 - \gamma_{0_3})$ is the deviation from the solution considered. The constant matrices $\mathbf{A}$ and $\mathbf{B}$ have the block diagonal form

$$\mathbf{A} = \begin{pmatrix} \mathbf{I} + \mathbf{J_{ss}} - \mathbf{J_{ns}} - \mathbf{J_{sn}} & \mathbf{J_{ns}} - \mathbf{J_{ss}} + mR_0((\boldsymbol{\gamma}_0,\boldsymbol{r_m}) - \boldsymbol{\gamma}_0\otimes\boldsymbol{r_m}) & 0\\ \mathbf{J_{sn}} - \mathbf{J_{ss}} + mR_0((\boldsymbol{r_m},\boldsymbol{\gamma}_0) - \boldsymbol{r_m}\otimes\boldsymbol{\gamma}_0) & I_0 + \mathbf{J_{ss}} + (m+m_0){R_0}^2(\boldsymbol{\gamma}_0^2 - \boldsymbol{\gamma}_0\otimes\boldsymbol{\gamma}_0) & 0\\ 0 & 0 & \mathbf{E}\end{pmatrix},$$

$$\mathbf{B} = \begin{pmatrix} \widehat{\boldsymbol{\Omega}} - mR_0R_m(\widetilde{\boldsymbol{\Omega}}_0(\boldsymbol{\gamma}_0\otimes\boldsymbol{\gamma}_0) + (\boldsymbol{\Omega}_0,\boldsymbol{\gamma}_0)\widetilde{\boldsymbol{\gamma}}_0 & 0 & mgR_m\widetilde{\boldsymbol{\gamma}}_0\\ -\mathbf{I}\widetilde{\boldsymbol{\Omega}}_0 - (m+m_0)R_0^2(\widetilde{\boldsymbol{\Omega}}_0(\boldsymbol{\gamma}_0\otimes\boldsymbol{\gamma}_0) + (\boldsymbol{\Omega}_0,\boldsymbol{\gamma}_0)\widetilde{\boldsymbol{\gamma}}_0 & 0 & 0\\ -\widetilde{\boldsymbol{\gamma}}_0 & 0 & 0\end{pmatrix},$$

where $\mathbf{E}$ is a 3×3 identity matrix, the matrices $\widetilde{\boldsymbol{\gamma}}_0$, $\widetilde{\boldsymbol{\Omega}}_0$ and $\widehat{\boldsymbol{\Omega}}$ are defined as

$$\widetilde{\boldsymbol{\gamma}}_{0_{ij}} = \varepsilon_{ijk}\boldsymbol{\gamma}_{0_k},\ \widetilde{\boldsymbol{\Omega}}_{0_{ij}} = \varepsilon_{ijk}\boldsymbol{\Omega}_{0_k},\ \widehat{\boldsymbol{\Omega}}_{ij} = \varepsilon_{ijk}(\mathbf{J_{ns}}\boldsymbol{\Omega}_0)_k,$$

and ε_{ijk} is the Levi-Civita symbol.

In order to determine whether this solution is stable, we need to find the roots of the characteristic equation of the system (4.15)

$$\det(\mu\mathbf{A} - \mathbf{B}) = 0. \tag{4.16}$$

In the general case, Eq. (4.16) has quite a complex form, therefore here (and in the sequel, in performing numerical calculations) we restrict ourselves to stability analysis for the given system parameters corresponding to the experimental specimen of the spherical robot described earlier in this paper. We assume that the missing dynamic parameters of the full-scale specimen are: $\boldsymbol{r_m} = (0, 0, 0.08)$, $j = 0.00011$. Furthermore, we restrict ourselves to considering the case when there is no spinning of the spherical shell at the point of contact with the plane, that is, we assume that $(\boldsymbol{\Omega}, \boldsymbol{\gamma}) = 0$. In this case the family of solutions (4.13) can be parameterized as follows:

$$\boldsymbol{\omega}_0 = (0, 0, 0),\ \boldsymbol{\Omega}_0 = (-\Omega_0 \sin(\delta),\ \Omega_0 \cos(\delta), 0),\ \boldsymbol{\gamma}_0 = (0, 0, 1). \tag{4.17}$$

Here $\Omega_0 = \frac{v}{R_0}$ defines the angular velocity of the spherical shell when the spherical robot is rolling in a straight line with velocity v, and the angle δ (as above) defines the direction of motion relative to the axis OX.

Substituting the parameter values into Eq. (4.16) taking into account the chosen parameterization (4.17), we obtain the following characteristic equation

$$\mu^5 \cdot (\mu^2 + 204.2205)(\mu^2 + 0.00829 \cdot \Omega_0^2 + 204.2205) = 0. \tag{4.18}$$

As can be seen from (4.18), the eigenvalues of the characteristic equation are not dependent on the angle δ, i.e., the direction of motion. Furthermore, they do not have a positive real component, no matter what the value of Ω_0 is. This suggests that there is no exponential instability of the solution. The presence of zero eigenvalues means that it is required to decompose the system (4.5) to higher orders in order to solve the problem of nonlinear stability.

Remark. Note that for the design of a spherical robot considered here the solution (4.14) degenerates into rotation of the spherical robot at the same place when the spherical shell and the internal moving platform rotate about the vertical axis with constant but different angular velocities $\boldsymbol{\Omega}_0$ and $\boldsymbol{\omega}_0$. For this reason, analysis of stability of these solutions is of no practical interest.

4.4. Control Along a Prescribed Trajectory

We now consider the problem of controlling the system under consideration as formulated in Section 2 of this paper. This problem is solved by means of an algorithm comprising the following steps.

1. We express the angular velocity $\boldsymbol{\Omega}$ in the form

$$\boldsymbol{\Omega} = \Omega_\alpha(t)\boldsymbol{\alpha} + \Omega_\beta(t)\boldsymbol{\beta} + \Omega_\gamma(t)\boldsymbol{\gamma}, \tag{4.19}$$

where $\Omega_\gamma(t)$ is a known function of time, and $\Omega_\alpha(t), \Omega_\beta(t)$ are expressed by means of the constraint equation (3.1) and the first of the kinematic equations (2.1) as follows

$$\Omega_\alpha(t) = \frac{\dot{y}(t)}{R_0}, \quad \Omega_\beta(t) = \frac{\dot{x}(t)}{R_0}.$$

2. We exclude the control torques $\boldsymbol{K}(t)$ from Eqs. (4.5) (by adding the first and the second equations of the system). As a result, together with the second kinematic equation (2.1) we get a closed nonautonomous system of differential equations

$$\begin{gathered}
(\mathbf{I} - J_{ns} + mR_0((\boldsymbol{r_m}, \boldsymbol{\gamma}) - \boldsymbol{r_m} \otimes \boldsymbol{\gamma}))\dot{\boldsymbol{\omega}} \\
+ (J_{ns} + I_0 + (m + m_0){R_0}^2(\boldsymbol{\gamma}^2 - \boldsymbol{\gamma} \otimes \boldsymbol{\gamma}) + mR_0((\boldsymbol{\gamma}, \boldsymbol{r_m}) - \boldsymbol{\gamma} \otimes \boldsymbol{r_m}))\dot{\boldsymbol{\Omega}} \\
= -\boldsymbol{\omega} \times (\mathbf{I}\boldsymbol{\omega} + I_0\boldsymbol{\Omega} + J_{ns}(\boldsymbol{\Omega} - \boldsymbol{\omega})) - mR_0\,(\boldsymbol{r_m} \times (\boldsymbol{\gamma} \times (\boldsymbol{\Omega} \times \boldsymbol{\omega}))) - mg(\boldsymbol{r_m} \times \boldsymbol{\gamma}) \\
-(m + m_0){R_0}^2(\boldsymbol{\gamma} \times (\boldsymbol{\gamma} \times (\boldsymbol{\Omega} \times \boldsymbol{\omega}))) - mR_0(\boldsymbol{\gamma} \times (\boldsymbol{\omega}(\boldsymbol{\omega}, \boldsymbol{r_m}) - \boldsymbol{r_m})) \\
\dot{\boldsymbol{\alpha}} = \boldsymbol{\alpha} \times \boldsymbol{\omega},\ \dot{\boldsymbol{\beta}} = \boldsymbol{\beta} \times \boldsymbol{\omega},\ \dot{\boldsymbol{\gamma}} = \boldsymbol{\gamma} \times \boldsymbol{\omega}.
\end{gathered} \tag{4.20}$$

Substituting (4.19) into the resulting equations and numerically integrating the system with the specified initial conditions $\boldsymbol{\alpha}(0)$, $\boldsymbol{\beta}(0)$, $\boldsymbol{\gamma}(0)$ and $\boldsymbol{\omega}(0)$ yields an explicit time dependence of the vectors $\boldsymbol{\alpha}$, $\boldsymbol{\beta}$, $\boldsymbol{\gamma}$ and $\boldsymbol{\omega}$.

3. Substituting the resulting solutions for $\boldsymbol{\alpha}(t)$, $\boldsymbol{\beta}(t)$, $\boldsymbol{\gamma}(t)$, $\boldsymbol{\omega}(t)$ into one of Eqs. (4.5), we find the time dependence of the control torques $\boldsymbol{K}(t)$.

In practice, this algorithm can be applied only hypothetically because under real-time conditions involving high-velocity motions the process of numerical integration takes quite a long time, which is critical for the control problems. Moreover, the resulting system is nonintegrable, hence there exists the probability of obtaining a chaotic solution, which requires a separate analysis.

Let us consider an example of determining control torques necessary for the spherical robot to move along the segment [0, 1] without rotation of the spherical shell about the vertical axis

$$x(t) = 0, \quad y(t) = -\frac{\sin(2\pi t)}{20\pi} + \frac{t}{10}, \quad \Omega_\gamma = 0. \tag{4.21}$$

The results of the numerical solution of the system (4.20) for the angular velocity of the moving platform $\boldsymbol{\omega}$ and the vector $\boldsymbol{\gamma}$ are shown in Figs. 3a and 3b. The corresponding time dependencies of the control torques required for the motion along the trajectory (4.21) are shown in Fig. 3c.

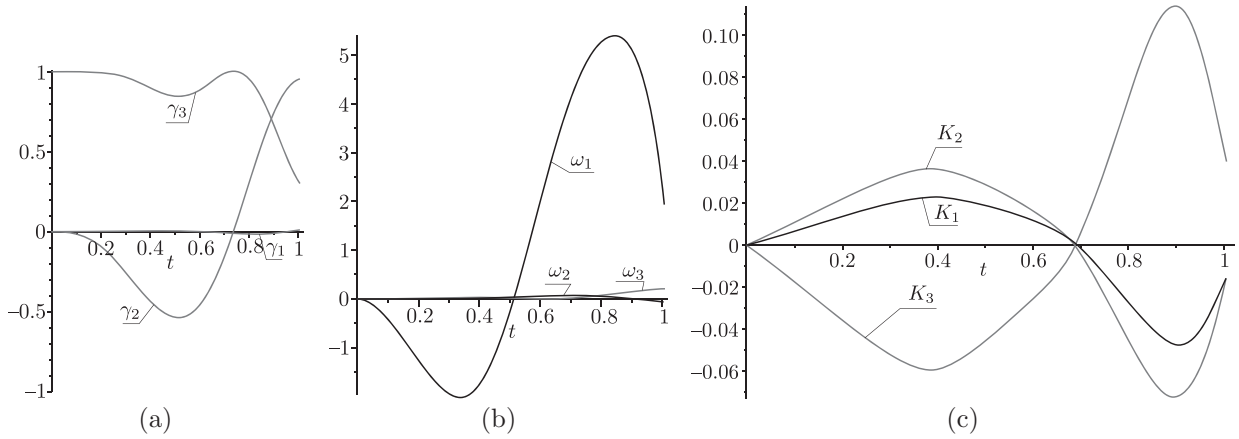

Fig. 3. Dependencies of $\boldsymbol{\gamma}(t)$ (a), $\boldsymbol{\omega}(t)$ (b) and $\boldsymbol{K}(t)$ (c) for spherical robot motion along the trajectory (4.21).

As seen from the graphs, neither the angular velocity of the moving platform $\boldsymbol{\omega}$ nor the vector components γ_1 and γ_2 are equal to zero at the endpoint. Consequently, after the spherical robot has moved in a straight line in accordance with the controls shown in Fig. 3c, it will not stop but will continue to move freely (in the general case, chaotically). The initial conditions for this motion will be the position and velocity of the platform and the spherical shell at the time of control deactivation. There are three ways to eliminate such effects.

1. Continue to control the system after the stop to make the spherical shell stay in place while the omniwheel platform will keep moving inside the stationary shell. In this case it is necessary to solve the system (4.20) under the condition $\boldsymbol{\Omega}(t) = \dot{\boldsymbol{\Omega}}(t) = 0$ in the time interval $t > T$ and to find the corresponding control $\boldsymbol{K}(t)$, $t > T$. However, the solution to (4.20) is likely to be divergent. The search for the solution to (4.20) and its analysis requires a separate study, which is outside of the scope of this paper.

2. Choose a dependence $\Omega_\gamma(t)$ or velocity of passage along the prescribed trajectory such that the position and velocity of the omniwheel platform at the final time $t = T$ correspond to a steady-state solution of the free system. In this case, after control deactivation the spherical robot will move in accordance with a steady-state solution (in a particular case, stand still). This method involves solving a variational problem with respect to the velocity of motion along the trajectory and/or the dependence $\boldsymbol{\Omega}_\gamma(t)$ and is quite laborious.

The third method is associated with control by means of gaits and is described in more detail in the next section.

5. CONTROL BY MEANS OF GAITS

This method consists in calculating the control actions with which the spherical robot will invariably move in accordance with a steady-state solution (in a particular case, stand still) at the initial and final instants of time. However, in this case the trajectory of motion of the spherical robot is not pre-determined. Here, the control problem is reduced to choosing a maneuver with which the final trajectory of motion of the spherical robot will meet the necessary requirements. An example of such control for a spherical robot with an internal Lagrange pendulum is given in [15]. We consider a similar algorithm of searching for a suitable maneuver that connects two straight-line motions (4.13).

Straight-line motions corresponding to the fixed points (4.13) can be parameterized by four variables: v — the velocity of motion in a straight line, δ — the angle between the straight line and the axis OX, Ω_γ — the angular velocity of spinning of the shell at the point of contact with the plane, and ψ — the constant precession angle that defines the orientation of the omniwheel platform during motion. Note that the other two Euler angles θ and φ are also constant in the case of straight-line motion and are defined by the vector $\boldsymbol{\gamma} \parallel \boldsymbol{r_m}$. These parameters relate to the vectors $\boldsymbol{\alpha}, \boldsymbol{\beta}, \boldsymbol{\gamma}$ and $\boldsymbol{\Omega}$ as follows:

$$\boldsymbol{\Omega} = \Omega_\gamma \boldsymbol{\gamma} + \frac{v}{R_0}(\cos(\delta)\boldsymbol{\beta} - \sin(\delta)\boldsymbol{\alpha}), \quad \operatorname{tg}(\psi) = -\frac{\beta_3}{\alpha_3}. \tag{5.1}$$

It is easy to show that the following proposition holds.

Proposition 4. *Let the spherical robot move along a straight line with the parameters $v_0, \delta_0, \Omega_{\gamma_0}, \psi_0$, with $t < 0$. In addition, when making a maneuver the vector $\boldsymbol{\gamma}$ and the value of ω_γ are specified functions of time*

$$\boldsymbol{\gamma} = \boldsymbol{\gamma}(t),\ \omega_\gamma = \omega_\gamma(t), t \in [0,\ T]$$

such that

$$\boldsymbol{\gamma}(0) = \boldsymbol{\gamma}(T) = \frac{\boldsymbol{r_m}}{|\boldsymbol{r_m}|},\ \dot{\boldsymbol{\gamma}}(0) = \dot{\boldsymbol{\gamma}}(T) = 0,\ \omega_\gamma(0) = \omega_\gamma(T) = 0.$$

Then, after making the maneuver (with $t > T$) the spherical robot will move in a straight line with the parameters $v_f, \delta_f, \Omega_{\gamma_f}, \psi_f$ related with the vectors $\boldsymbol{\alpha}(T), \boldsymbol{\beta}(T), \boldsymbol{\Omega}(T)$ by ratios similar to (5.1)*. The time dependencies $\boldsymbol{\alpha}(t), \boldsymbol{\beta}(t), \boldsymbol{\Omega}(t)$ are found by solving the first three equations of the system* (4.20) *in which the vector $\boldsymbol{\omega}$ is a known function of time expressed in terms of $\boldsymbol{\gamma}(t)$ and $\omega_\gamma(t)$ as follows:*

$$\boldsymbol{\omega}(t) = \boldsymbol{\gamma}(t)\omega_\gamma(t) + \dot{\boldsymbol{\gamma}}(t) \times \boldsymbol{\gamma}(t).$$

The controls required to realize this maneuver can be obtained by substituting $\boldsymbol{\omega}(t), \boldsymbol{\Omega}(t)$ and $\boldsymbol{\gamma}(t)$ into one of Eqs. (4.5)*, and the explicit form of the trajectory of the spherical robot connecting two straight-line motions can be obtained by integrating the first of the kinematic equations* (2.1)*.*

As an example, let us consider the spherical robot controls required to accelerate from rest and to make a turn during straight-line motion. We express the vector $\boldsymbol{\gamma}$ defining the maneuver (gait) as

$$\boldsymbol{\gamma}(t) = (\sin(\theta(t))\cos(\varphi(t)),\ \sin(\theta(t))\sin(\varphi(t)),\ \cos(\theta(t)))\,,$$

where the orientation of the moving platform during the maneuver is defined by the Euler angles $\varphi(t)$ and $\theta(t)$. We choose the dependencies $\varphi(t), \theta(t), \omega_\gamma(t)$ for both maneuvers as

$$\theta(t) = \theta_{max}\sin^2(\pi t),\ \varphi(t) = \varphi_0 = 0,\ \omega_\gamma(t) = 0,\ t \in [0,\ 1], \tag{5.2}$$

where θ_{max} for the purpose of numerical calculations is assumed to be $\theta_{max} = 0.2$. The only difference between these two maneuvers lies in the different initial conditions. Accelerating from rest corresponds to the following initial conditions

$$\Omega_0 = 0,\ \boldsymbol{\alpha}_0 = (1,\ 0,\ 0),\ \boldsymbol{\beta}_0 = (0,\ 1,\ 0), \tag{5.3}$$

while making a turn from initially straight-line motion corresponds to the following initial conditions:

$$\boldsymbol{\Omega}_0 = (-1,\ 0,\ 0),\ \boldsymbol{\alpha}_0 = (1,\ 0,\ 0),\ \boldsymbol{\beta}_0 = (0,\ 1,\ 0). \tag{5.4}$$

The results of the numerical solution of the system of Eqs. (4.20) for the maneuver (5.2) with the initial conditions (5.3) and (5.4) are shown in Fig. 4 and Fig. 5, respectively.

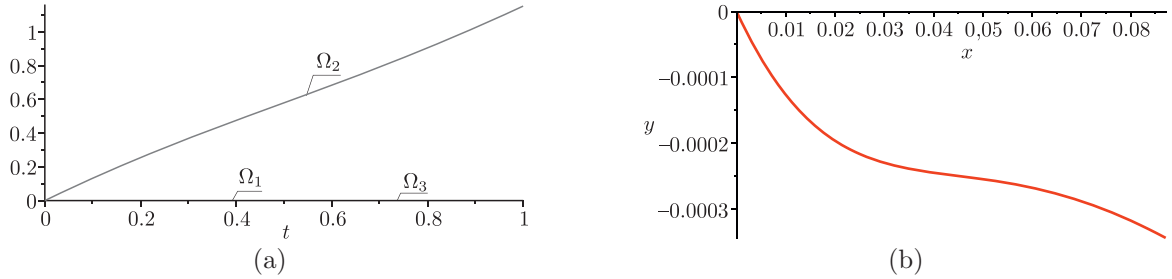

Fig. 4. The angular velocity $\boldsymbol{\Omega}(t)$ (a) and the trajectory of motion $y(x)$ (b) of the spherical robot during acceleration in accordance with the initial conditions (5.3).

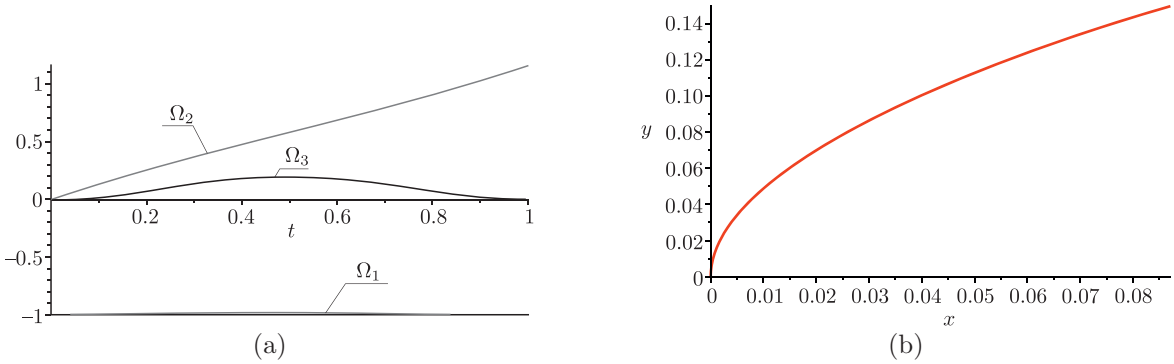

Fig. 5. The angular velocity $\boldsymbol{\Omega}(t)$ (a) and the trajectory of motion $y(x)$ (b) of the spherical robot when making a turn in accordance with the initial conditions (5.4).

As shown in Fig. 4, since the design of the omniwheel platform is not axially symmetric, changing $\boldsymbol{\gamma}(t)$ in the vertical plane on the Poisson sphere ($\varphi = \text{const}$) results in curvilinear, albeit quite close to rectilinear, motion of the spherical robot. This is what makes this system different from a spherical robot with the Lagrange pendulum, where such controls lead to purely linear motion.

Using the above procedure we can obtain the (numerical) dependence of the parameters of the final motion on the parameters of the initial motion and the maneuver

$$\boldsymbol{p}_f = \boldsymbol{f}(\boldsymbol{p}_0,\ \theta_{max},\ \varphi_0), \tag{5.5}$$

where the notation $\boldsymbol{p} = (v, \delta, \Omega_\gamma, \psi)$ is introduced. However, the reverse dependence is usually required in practice to find control parameters depending on the desired final motion. Inverting any two equations of the system (5.5) (for example, for v and δ), we can obtain the (numerical) dependence of θ_{max} and φ_0 on the parameters of the initial and final motions

$$(\theta_{max},\ \varphi_0) = \widetilde{\boldsymbol{f}}(\boldsymbol{p}_0,\ v_f,\ \delta_f). \tag{5.6}$$

This dependence includes only two parameters of the final motion, while the remaining two parameters $(\Omega_{\gamma_f}, \psi_f)$ are found from Eqs. (5.5). Note that the chosen pair of Eqs. (5.5) is not always solvable for θ_{max} and φ_0. The conditions of their solvability impose restrictions on the possible maneuvers accomplished by means of the dependence (5.2).

Using the numerical dependence (5.6), we can define the maneuver parameters θ_{max} and φ_0 that will allow one to make a turn by a predetermined angle with acceleration (deceleration) to the desired velocity. The final motion parameters $(\Omega_{\gamma_f}, \psi_f)$ are not controlled. That is, after the maneuver the omniwheel platform will move with a different orientation (relative to the initial one), and the shell may acquire some rotation about the vertical axis.

Remark. For a fully controlled maneuver, we need to consider the four-parameter time dependence $\boldsymbol{\gamma}(t), \omega_\gamma(t)$ and ensure that equations such as (5.5) are solvable for input parameters.

6. CONCLUSION

In conclusion, we summarize the main results of this paper and the questions that remain to be answered.

- The problem of controlling the motion of a spherical robot in the kinematic (quasi-static) formulation has been solved.
- It has been proven that in the framework of the kinematic (quasi-static) model the trajectory of a spherical robot with an internal omniwheel platform with constant control actions (rotational velocities of the omniwheels) is a circle or a straight line.
- A method for determining the position of the center of mass of the omniwheel platform based on experimental determination of the radii of curvature of trajectories during motion with two different constant control actions has been developed. This allows one, in particular, to create a theory of spherical robot control taking into account possible mass redistribution inside the spherical robot (for example, when changing the payload, etc.).
- An experimental validation of the theoretical results obtained in the framework of the kinematic model has been conducted. It has been shown that at low speeds this model is in satisfactory agreement with experimental results.
- Equations of dynamics of a spherical robot with an internal omniwheel platform have been obtained in the framework of the nonholonomic model. First integrals of motion for these equations, and all the fixed points of the reduced system corresponding to the motion of the spherical robot in a straight line or in a circle have been found.
- The stability of free straight-line motion of a spherical robot in the framework of linear approximation with fixed parameters of the spherical robot has been investigated. It would be interesting to analyze the stability of this solution as a function of parameters of the spherical robot. It would be also interesting to analyze the stability of free motion in a circle.
- A motion planning algorithm for a spherical robot has been developed. A shortcoming of this algorithm is that after the end of rolling along a prescribed trajectory (and control deactivation) the spherical robot continues its free motion, which in the general case is chaotic.
- In order to eliminate this shortcoming, a numerical algorithm for constructing elementary maneuvers (gaits) for transition from one steady-state motion to another has been developed. This algorithm has been illustrated by the acceleration and turning of the spherical robot during initially straight-line motion.

7. ACKNOWLEDGMENTS

The authors thank A. V. Borisov and I. S. Mamaev for fruitful discussions of the results obtained.

This work is supported by the Russian Science Foundation under grant 14-50-00005 and performed in Steklov Mathematical Institute of Russian Academy of Sciences.

REFERENCES

1. Kilin, A. A., The Dynamics of Chaplygin Ball: The Qualitative and Computer Analysis, *Regul. Chaotic Dyn.,* 2001, vol. 6, no. 3, pp. 291–306.
2. Borisov, A. V., Mamaev, I. S., and Kilin, A. A., The Rolling Motion of a Ball on a Surface: New Integrals and Hierarchy of Dynamics, *Regul. Chaotic Dyn.,* 2002, vol. 7, no. 2, pp. 201–219.
3. Chase, R. and Pandya, A., A Review of Active Mechanical Driving Principles of Spherical Robots, *Robotics,* 2012, vol. 1, no. 1, pp. 3–23.
4. Crossley, V. A., *A Literature Review on the Design of Spherical Rolling Robots,* Pittsburgh, Pa., 2006.
5. Ylikorpi, T. and Suomela, J., Ball-Shaped Robots, in *Climbing and Walking Robots: Towards New Applications,* H. Zhang (Ed.), Vienna: InTech, 2007.
6. *Mobile Robots: Ball-Shaped Robot and Wheel Robot,* A. V. Borisov, I. S. Mamaev, Yu. L. Karavaev (Eds.), Izhevsk: R&C Dynamics, Institute of Computer Science, 2013 (Russian).
7. Borisov, A. V., Kilin, A. A., and Mamaev, I. S., An Omni-Wheel Vehicle on a Plane and a Sphere, *Rus. J. Nonlin. Dyn.,* 2011, vol. 7, no. 4, pp. 785–801 (Russian).
8. Chen, W.-H., Chen, Ch.-P., Yu, W.-Sh., Lin, Ch.-H., and Lin, P.-Ch., Design and Implementation of an Omnidirectional Spherical Robot Omnicron, in *IEEE/ASME Internat. Conf. on Advanced Intelligent Mechatronics (Kachsiung, Taiwan, 2012),* pp. 719–724.
9. Borisov, A. V., Kilin, A. A., and Mamaev, I. S., How To Control Chaplygin's Sphere Using Rotors, *Regul. Chaotic Dyn.,* 2012, vol. 17, nos. 3–4, pp. 258–272.
10. Borisov, A. V., Kilin, A. A., and Mamaev, I. S., How To Control Chaplygin's Sphere Using Rotors: 2, *Regul. Chaotic Dyn.,* 2013, vol. 18, nos. 1–2, pp. 144–158.
11. Svinin, M., Morinaga, A., and Yamamoto, M., On the Dynamic Model and Motion Planning for a Spherical Rolling Robot Actuated by Orthogonal Internal Rotors, *Regul. Chaotic Dyn.,* 2013, vol. 18, nos. 1–2, pp. 126–143.
12. Morinaga, A., Svinin, M., and Yamamoto, M., A Motion Planning Strategy for a Spherical Rolling Robot Driven by Two Internal Rotors, *IEEE Trans. on Robotics,* 2014, vol. 30, no. 4, pp. 993–1002.
13. Svinin, M., Morinaga, A., and Yamamoto, M., On the Dynamic Model and Motion Planning for a Class of Spherical Rolling Robots, in *Proc. of the IEEE Internat. Conf. on Robotics and Automation (ICRA, 14–18 May, 2012),* pp. 3226–3231.
14. Kazakov, A. O., Strange Attractors and Mixed Dynamics in the Problem of an Unbalanced Rubber Ball Rolling on a Plane, *Regul. Chaotic Dyn.,* 2013, vol. 18, no. 5, pp. 508–520.
15. Ivanova, T. B. and Pivovarova, E. N., Dynamics and Control of a Spherical Robot with an Axisymmetric Pendulum Actuator, *Rus. J. Nonlin. Dyn.,* 2013, vol. 9, no. 3, pp. 507–520 (Russian).
16. Koshiyama, A. and Yamafuji, K., Design and Control of an All-Direction Steering Type Mobile Robot, *Int. J. Robot. Res.,* 1993, vol. 12, no. 5, pp. 411–419.
17. Balandin, D. V., Komarov, M. A., and Osipov, G. V., A Motion Control for a Spherical Robot with Pendulum Drive, *J. Comput. Sys. Sc. Int.,* 2013, vol. 52, no. 4, pp. 650–663; see also: *Izv. Ross. Akad. Nauk. Teor. Sist. Upr.,* 2013, no. 4, pp. 150–163.
18. Kayacan, E., Bayraktaroglu, Z. Y., and Saeys, W., Modeling and Control of a Spherical Rolling Robot: A Decoupled Dynamics Approach, *Robotica,* 2012, vol. 30, no. 12, pp. 671–680.
19. Yoon, J.-C., Ahn, S.-S., and Lee, Y.-J., Spherical Robot with New Type of Two-Pendulum Driving Mechanism, in *Proc. 15th IEEE Internat. Conf. on Intelligent Engineering Systems (INES) (Poprad, High Tatras, Slovakia, 2011),* pp. 275–279.
20. Zhao, B., Li, M., Yu, H., Hu, H., and Sun, L., Dynamics and Motion Control of a Two Pendulums Driven Spherical Robot, in *Proc. of the 2010 IEEE/RSJ Internat. Conf. on Intelligent Robots and Systems (IROS) (Taipei, Taiwan, October 2010),* pp. 147–153.
21. Bolsinov, A. V., Borisov, A. V., and Mamaev, I. S., Rolling of a Ball without Spinning on a Plane: The Absence of an Invariant Measure in a System with a Complete Set of Integrals, *Regul. Chaotic Dyn.,* 2012, vol. 17, no. 6, pp. 571–579.
22. Borisov, A. V., Fedorov, Yu. N., and Mamaev, I. S., Chaplygin Ball over a Fixed Sphere: An Explicit Integration, *Regul. Chaotic Dyn.,* 2008, vol. 13, no. 6, pp. 557–571.
23. Borisov, A. V. and Mamaev, I. S., Rolling of a Non-Homogeneous Ball over a Sphere without Slipping and Twisting, *Regul. Chaotic Dyn.,* 2007, vol. 12, no. 2, pp. 153–159.
24. Borisov, A. V. and Mamaev, I. S., Isomorphism and Hamilton Representation of Some Nonholonomic Systems, *Siberian Math. J.,* 2007, vol. 48, no. 1, pp. 26–36; see also: *Sibirsk. Mat. Zh.,* 2007, vol. 48, no. 1, pp. 33–45.
25. Ahn, S.-S. and Lee, Y.-J., Novel Spherical Robot with Hybrid Pendulum Driving Mechanism, *Adv. Mech. Eng.,* 2014, vol. 2014, 456727, 14 pp.
26. Forbes, J. R., Barfoot, T. D., and Damaren, Ch. J., Dynamic Modeling and Stability Analysis of a Power-Generating Tumbleweed Rover, *Multibody Syst. Dyn.,* 2010, vol. 24, no. 4, pp. 413–439.
27. Hartl, A. E. and Mazzoleni, A. P., Dynamic Modeling of a Wind-Driven Tumbleweed Rover Including Atmospheric Effects, *J. of Spacecraft and Rockets,* 2010, vol. 47, no. 3, pp. 493–502.

28. Hartl, A. E. and Mazzoleni, A. P., Parametric Study of Spherical Rovers Crossing a Valley, *J. Guid. Control Dynam.,* 2008, vol. 31, no. 3, pp. 775–779.
29. Hogan, F. R. and Forbes, J. R., Modeling of Spherical Robots Rolling on Generic Surfaces, *Multibody Syst. Dyn.,* 2014, 19 pp.
30. Hogan, F. R., Forbes, J. R., and Barfoot, T. D., Rolling Stability of a Power-Generating Tumbleweed Rover, *J. of Spacecraft and Rockets,* 2014, vol. 51, no. 6, pp. 1895–1906.
31. Lee, J. and Park, W., Design and Path Planning for a Spherical Rolling Robot, in *ASME Internat. Mechanical Engineering Congress and Exposition (San Diego, Calif., Nov. 15–21, 2013): Vol. 4A. Dynamics, Vibration and Control,* IMECE2013-64994, 8 pp.
32. Yu, T., Sun, H., Jia, Q., Zhang, Y., and Zhao, W., Stabilization and Control of a Spherical Robot on an Inclined Plane, *Res. J. Appl. Sci. Eng. Technology,* 2013, vol. 5, no. 6, pp. 2289–2296.
33. Kilin, A. A. and Karavaev, Yu. L., The Kinematic Control Model for a Spherical Robot with an Unbalanced Internal Omniwheel Platform, *Rus. J. Nonlin. Dyn.,* 2014, vol. 10, no. 4, pp. 497–511 (Russian).
34. Borisov, A. V., Kilin, A. A., and Mamaev, I. S., Generalized Chaplygin's Transformation and Explicit Integration of a System with a Spherical Support, *Regul. Chaotic Dyn.,* 2012, vol. 17, no. 2, pp. 170–190.
35. Borisov, A. V., Kilin, A. A., and Mamaev, I. S., Rolling of a Homogeneous Ball over a Dynamically Asymmetric Sphere, *Regul. Chaotic Dyn.,* 2011, vol. 16, no. 5, pp. 465–483.
36. Borisov, A. V. and Mamaev, I. S., *Rigid Body Dynamics: Hamiltonian Methods, Integrability, Chaos,* Izhevsk: R&C Dynamics, Institute of Computer Science, 2005 (Russian).
37. Kilin, A. A., Karavaev, Yu. L., and Klekovkin, A. V., Kinematic Control of a High Manoeuvrable Mobile Spherical Robot with Internal Omni-Wheeled Platform, *Rus. J. Nonlin. Dyn.,* 2014, vol. 10, no. 1, pp. 113–126 (Russian).
38. Borisov, A. V. and Mamaev, I. S., Rolling of a Non-Homogeneous Ball over a Sphere without Slipping and Twisting, *Regul. Chaotic Dyn.,* 2007, vol. 12, no. 2, pp. 153–159.
39. Borisov, A. V., Mamaev, I. S., and Bizyaev, I. A., The Hierarchy of Dynamics of a Rigid Body Rolling without Slipping and Spinning on a Plane and a Sphere, *Regul. Chaotic Dyn.,* 2013, vol. 8, no. 3, pp. 277–328; see also: *Rus. J. Nonlin. Dyn.,* 2013, vol. 9, no. 2, pp. 141–202.
40. Bolsinov, A. V., Borisov, A. V., and Mamaev, I. S., Rolling of a Ball without Spinning on a Plane: The Absence of an Invariant Measure in a System with a Complete Set of Integrals, *Regul. Chaotic Dyn.,* 2012, vol. 17, no. 6, pp. 571–579; see also: *Rus. J. Nonlin. Dyn.,* 2012, vol. 8, no. 3, pp. 605–616.
41. Koiller, J. and Ehlers, K. M., Rubber Rolling over a Sphere, *Regul. Chaotic Dyn.,* 2007, vol. 12, no. 2, pp. 127–152.
42. Borisov, A. V., Kazakov, A. O., and Sataev, I. R., The Reversal and Chaotic Attractor in the Nonholonomic Model of Chaplygin's Top, *Regul. Chaotic Dyn.,* 2014, vol. 19, no. 6, pp. 718–733.
43. Borisov, A. V., Kazakov, A. O., and Kuznetsov, S. P., Nonlinear Dynamics of the Rattleback: A Nonholonomic Model, *Physics-Uspekhi,* 2014, vol. 57, no. 5, pp. 453–460; see also: *Uspekhi Fiz. Nauk,* 2014, vol. 184, no. 5, pp. 493–500.
44. Borisov, A. V. and Mamaev, I. S., Strange Attractors in Rattleback Dynamics, *Physics-Uspekhi,* 2003, vol. 46, no. 4, pp. 393–403; see also: *Uspekhi Fiz. Nauk,* 2003, vol. 173, no. 4, pp. 407–418.
45. Borisov, A. V., Kilin, A. A., Mamaev, I. S., New Effects in Dynamics of Rattlebacks, *Dokl. Phys.,* 2006, vol. 51, no. 5, pp. 272–275; see also: *Dokl. Akad. Nauk,* 2006, vol. 408, no. 2, pp. 192–195.
46. Vetchanin, E. V., Mamaev, I. S., and Tenenev, V. A., The Self-Propulsion of a Body with Moving Internal Masses in a Viscous Fluid, *Regul. Chaotic Dyn.,* 2013, vol. 18, nos. 1–2, pp. 100–117.
47. Bolotin, S. V. and Popova, T. V., On the Motion of a Mechanical System inside a Rolling Ball, *Regul. Chaotic Dyn.,* 2013, vol. 18, nos. 1–2, pp. 159–165.
48. Rutstam, N., High Frequency Behavior of a Rolling Ball and Simplification of the Separation Equation, *Regul. Chaotic Dyn.,* 2013, vol. 18, no. 3, pp. 226–236.
49. Borisov, A. V. and Mamaev, I. S., Topological Analysis of an Integrable System Related to the Rolling of a Ball on a Sphere, *Regul. Chaotic Dyn.,* 2013, vol. 18, no. 4, pp. 356–371.
50. Borisov, A. V. and Mamaev, I. S., The Dynamics of the Chaplygin Ball with a Fluid-Filled Cavity, *Regul. Chaotic Dyn.,* 2013, vol. 18, no. 5, pp. 490–496.
51. Gonchenko, A. S., Gonchenko, S. V., and Kazakov, A. O., Richness of Chaotic Dynamics in Nonholonomic Models of a Celtic Stone, *Regul. Chaotic Dyn.,* 2013, vol. 18, no. 5, pp. 521–538.
52. Borisov, A. V., Kilin, A. A., and Mamaev, I. S., The Problem of Drift and Recurrence for the Rolling Chaplygin Ball, *Regul. Chaotic Dyn.,* 2013, vol. 18, no. 6, pp. 832–859.
53. Takano, H., Spin Reversal of a Rattleback with Viscous Friction, *Regul. Chaotic Dyn.,* 2014, vol. 19, no. 1, pp. 81–99.
54. Mamaev, I. S. and Ivanova, T. B., The Dynamics of a Rigid Body with a Sharp Edge in Contact with an Inclined Surface in the Presence of Dry Friction, *Regul. Chaotic Dyn.,* 2014, vol. 19, no. 1, pp. 116–139.
55. Ivanova, T. B. and Pivovarova, E. N., Comments on the Paper by A. V. Borisov, A. A. Kilin, I. S. Mamaev "How To Control the Chaplygin Ball Using Rotors: 2", *Regul. Chaotic Dyn.,* 2014, vol. 19, no. 1, pp. 140–143.

56. Bizyaev, I. A., Borisov, A. V., and Mamaev, I. S., The Dynamics of Nonholonomic Systems Consisting of a Spherical Shell with a Moving Rigid Body Inside, *Regul. Chaotic Dyn.,* 2014, vol. 19, no. 2, pp. 198–213.
57. Burlakov, D. and Treschev, D., A Rigid Body on a Surface with Random Roughness, *Regul. Chaotic Dyn.,* 2014, vol. 18, no. 3, pp. 296–309.
58. Borisov, A. V., Erdakova, N. N., Ivanova, T. B., and Mamaev, I. S., The Dynamics of a Body with an Axisymmetric Base Sliding on a Rough Plane, *Regul. Chaotic Dyn.,* 2014, vol. 19, no. 6, pp. 607–634.
59. Borisov, A. V., Mamaev, I. S., and Kilin, A. A., Stability of Steady Rotations in the Nonholonomic Routh Problem, *Regul. Chaotic Dyn.,* 2008, vol. 13, no. 4, pp. 239–249.